



## Top-down fabrication of horizontally-aligned gallium nitride nanowire arrays for sensor development<sup>☆</sup>



Guannan Liu<sup>a,b</sup>, Baomei Wen<sup>b,c</sup>, Ting Xie<sup>a,b</sup>, Audie Castillo<sup>b,c</sup>, Jong-Yong Ha<sup>a,b</sup>, Nichole Sullivan<sup>c</sup>, Ratan Debnath<sup>b,c</sup>, Albert Davydov<sup>b</sup>, Martin Peckerar<sup>a</sup>, Abhishek Motayed<sup>a,b,c,\*</sup>

<sup>a</sup> Department of Electrical and Computer Engineering, University of Maryland, College Park, MD 20742, USA

<sup>b</sup> Material Measurement Laboratory, National Institute of Standards and Technology, Gaithersburg, MD 20899, USA

<sup>c</sup> N5 Sensors, Inc., 9610 Medical Center Drive, Suite 200, Rockville, MD 20850, USA

### ARTICLE INFO

#### Article history:

Received 14 November 2014

Received in revised form 4 August 2015

Accepted 7 August 2015

Available online 12 August 2015

#### Keywords:

Gallium nitride

Nanowire

Top-down approach

Surface treatment

Sensors

### ABSTRACT

This paper demonstrates a high-throughput fabrication method of gallium nitride (GaN) nanowire (NW) and sub-micron wire (SMW) arrays using a combination of projection lithography, plasma etching, and post-plasma wet etching techniques. Photoluminescence (PL), field emission scanning electron microscopy (FESEM), and I–V measurements were used to characterize the GaN NW/SMW devices. These NWs/SMWs can be used to create highly-sensitive and selective conductometric chemical/bio-sensors.

The length and width of the wires can be precisely customized. The length of the NW/SMW varied from 5  $\mu\text{m}$  to 5 mm and the width ranges from 100 nm to 500 nm. Such comprehensive control in the geometry of a wire is difficult to achieve with other fabrication methods. The post-plasma KOH wet etching greatly reduces the surface roughness of the GaN NW/SMW as well as the performance of devices. Complementary metal-oxide-semiconductor (CMOS) and micro-electro-mechanical system (MEMS) devices can be incorporated with GaN NW/SMW arrays on a single chip using this top-down fabrication method.

© 2015 Elsevier B.V. All rights reserved.

## 1. Introduction

Gallium nitride (GaN) is a versatile semiconductor used in optical devices (light-emitting diodes, laser diodes, UV sensors) and in power electronics (power switches, RF devices, and high power transistors) [1]. Due to its direct band gap and chemical and thermal stability, GaN nanowires (NWs) are gaining significant importance as chemical sensor elements [2–4].

To date, most of GaN NWs devices are fabricated using chemical vapor deposition growth with a follow-up detachment from the substrate and individual on-chip alignment. Due to the variation in morphology, dimensions, doping, and crystal quality, it is hard to control the quality of NWs grown via the bottom-up methods [5]. Besides, variations from a multi-step pick-and-plate fabrication process result in a low yield of functioning devices. Thus, such a process has low large-area integration capabilities, rendering mass-manufacturing

challenging. An alternative approach to overcome these drawbacks is the top-down fabrication, in which NWs are patterned on a uniform thin-film using standard lithography and etching. Vertically-aligned semiconductor NWs (nanorods, nanopillars or nanocolumns) have been demonstrated by such top-down methods [6–10]. The heights of these nanostructures are limited by the thickness of the starting thin-film material, and they often exhibit tapering as a result of etching. On the contrary, horizontally-aligned NWs can be fabricated without any length limitations. For photodetectors and photovoltaic devices, vertically-aligned nanowires represent a high efficiency platform, whereas for chemical sensors horizontally-aligned nanowires are the optimal choice [11–13]. Due to its inherent inertness to most wet chemical etches, GaN nanostructures are commonly produced using dry etch techniques [8]. However, high-aspect ratio GaN structures achieved by plasma etching are often associated with extensive side wall damage, result in lower performance of the device [14]. Therefore, producing damage-free nitride structures with a precisely-defined geometry over large area remains a challenge.

By combining deep-UV projection lithography and inductively-coupled plasma (ICP) etching, this paper demonstrates horizontally-aligned NWs etched from a GaN thin film grown on sapphire. Since the rough and tapered NW sidewalls due to dry etching create leakage current and limit NW performance [14], a post ICP potassium hydroxide (KOH) wet etching procedure was developed to smooth the NW walls.

<sup>☆</sup> Certain commercial equipment, instruments, or materials are identified in this paper in order to specify the experimental procedure adequately. Such identification is not intended to imply recommendation or endorsement by the National Institute of Standards and Technology, nor is it intended to imply that the materials or equipment identified are necessarily the best available for the purpose.

\* Corresponding author at: Department of Electrical and Computer Engineering, University of Maryland, College Park, MD 20742, USA.

E-mail address: [abhishek.motayed@nist.gov](mailto:abhishek.motayed@nist.gov) (A. Motayed).

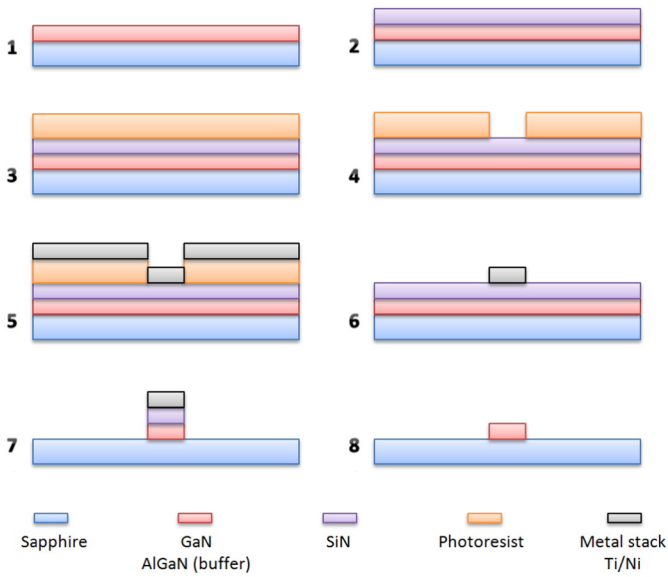


**Fig. 1.** Schematic representation of the nanowire fabrication process flow. (1) RCA cleaning of GaN on sapphire wafer, (2) SiN etch-mask deposited using PECVD, (3) spin-coating of photo-resist stack of LOR3A and Ultra-I, (4) lithography and development, (5) metal deposition by e-beam evaporator, (6) lift-off in 1165 photo-resist remover, (7) ICP etching to transfer the pattern on GaN, (8) HF etching, RIE etching to remove metal and SiN etch masks, followed by subsequent KOH wet etch treatment.

The KOH etching also allows us to control the final shape and dimensions of the NWs. The PL and current–voltage (I–V) results verify the improved performance resulting from the KOH treatment.

The top–down approach described here can potentially enable GaN NW and SMW to be integrated with LED, micro-pumps, and micro heaters for system-on-chip development [15–20]. Different types of sensors such as chemical, gas and bio sensors can be fabricated using the top–down method reported here.

## 2. Fabrication

Two different thicknesses of commercial intrinsic GaN epitaxial layers (NTT Advanced Technology) grown on c-plane sapphire were used in this study: 3  $\mu\text{m}$  thick GaN films were used for characterization of the etch rate of ICP dry etching, optimization of wet etching and measurements of PL spectra; 1  $\mu\text{m}$  thick GaN films were used in the optimization of the wet etching process as well as in I–V characterization. AlGaIn is a buffer layer widely used to compensate lattice mismatch and reduce stress in the growing film, and thereby improves the crystalline quality of GaN on sapphire. In our experiment, a 500 nm AlGaIn

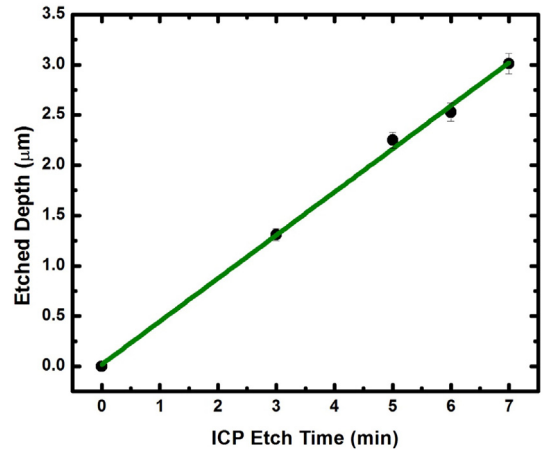


**Fig. 3.** ICP etch depth as a function of the etch time. The original data are shown by black dots, and a linear fit to the data shown by the solid green line. (For interpretation of the references to color in this figure legend, the reader is referred to the web version of this article.)

layer was used between the GaN and sapphire substrate. A silicon nitride (SiN) passivation layer with thickness of 50 nm was deposited by plasma enhanced chemical vapor deposition (PECVD). This layer prevents metal penetration into the bulk GaN. A bi-layer stack of photoresist (MicroChem LOR3A and Ultra-i) was spun onto the wafer for photolithography patterning. The 570  $\text{mJ}/\text{cm}^2$  stepper lithography dose was optimized for the fabrication process.

A bi-layer metal stack (50 nm Ti and 120 nm Ni) was deposited by e-beam evaporator (Denton Infinity 22) and lifted-off. This was followed by ICP etching (Oxford Plasmalab 100) with a combination gases ( $\text{Cl}/\text{N}_2/\text{Ar}$  25/5/1 sccm) at 40  $^\circ\text{C}$  temperature, 300 W RF power and 800 W ICP power. After removal of Ti/Ni metal shadow mask and SiN, potassium hydroxide (KOH) wet etching was studied at various temperatures (40  $^\circ\text{C}$ , 60  $^\circ\text{C}$ , and 80  $^\circ\text{C}$ ) and in different solvents (deionized water, isopropanol, and ethylene glycol), and for different etching times from 10 min to 5 h. The fabrication steps for NW formation are shown in Fig. 1. PL measurements and SEM imaging were conducted before and after KOH etching as well as on the control sample (pristine GaN film). The optimized condition of KOH treatment (10% KOH in ethylene glycol etching for 2 h at 80  $^\circ\text{C}$ ) was used on NWs. An ohmic contact metal stack (Ti/Al/Ti/Au) was deposited by e-beam evaporation for I–V characterization of the samples. The electrical properties of the no KOH treatment control group and a 2 h KOH etched group with different length NWs were studied. Due to the highly resistive property of intrinsic GaN, I–V measurements were conducted under UV (355 nm wavelength, 48  $\mu\text{W}/\text{cm}^2$  intensity) illumination. The width of both

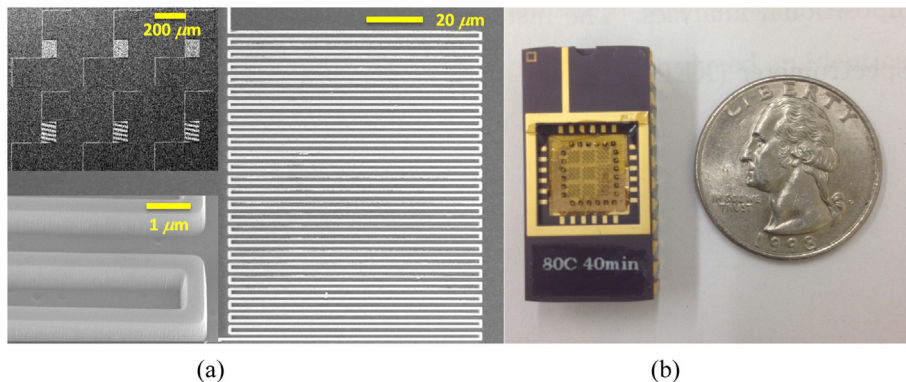


**Fig. 2.** (a) SEM image of single nanowire device. The total length is 5000  $\mu\text{m}$  and width of 500 nm. The upper inset shows the identical NW arrays. The lower inset shows a higher magnification SEM image of the same nanowire with 30 $^\circ$  tilt. (b) Final packaged device for photoconductance testing, a single die shown in the inset contains 81 NWs devices.

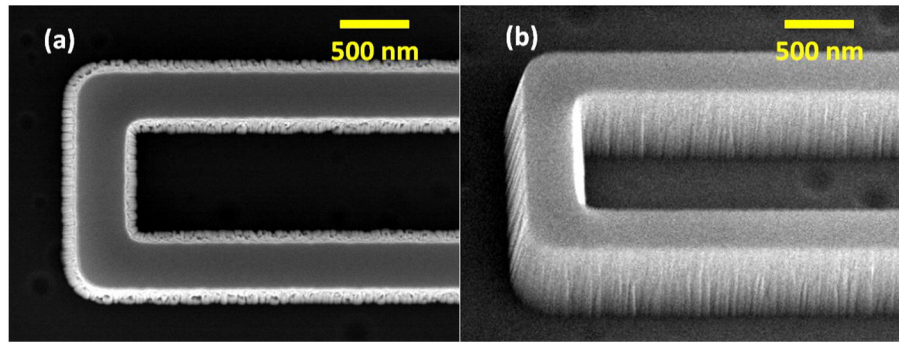


Fig. 4. SEM images of a nanowire section after ICP etch. (a) plan-view, (b) 45° tilted. The top surface appears smooth, however sidewall damage is evident.

multiple parallel NWs and single meander-shape NW arrays presented in this paper was 500 nm. By stepper lithography (ASML PAS5500) optimization, we were able to pattern MWs with width ranging from 200 nm to 300 nm. The final width after KOH wet etching was 100 nm.

### 3. Results and discussion

Fig. 2(a) shows SEM image of the longest length (5000  $\mu\text{m}$ ) wire in the meander-shape. The upper inset of Fig. 2(a) shows a low magnification image of 6 identical NWs. The lower inset of Fig. 2(a) shows a high magnification of a NW. The wire bonded NWs in a chip carrier for IV and photoconductance measurement are shown in Fig. 2(b). On a single chip, the total 9 groups of NW arrays with length range from 10  $\mu\text{m}$  to 5000  $\mu\text{m}$  were fabricated. And within each group, there are 9 identical NWs arranged in a  $3 \times 3$  matrix.

Several GaN layers (3  $\mu\text{m}$  thickness) were ICP etched for different times to calibrate the etch rate. The etched thickness was measured by a profilometer and the data summary is shown in Fig. 3. Black dots show the original data, and the regression linearization analysis (green line) gives the dry etching rate of 428.9 nm/min. Based on this rate, an 3 min etching was performed on the 1  $\mu\text{m}$  GaN/500 nm AlGaIn films to fabricate the nanowire devices.

Both top view and tilted SEM images of NWs after ICP etching are shown in Fig. 4. The vertical texture on the sidewalls formed by plasma bombardment is clearly seen in this figure. To remove the surface defects, KOH wet etching methods are explored with different etching temperatures, solvent compositions and times.

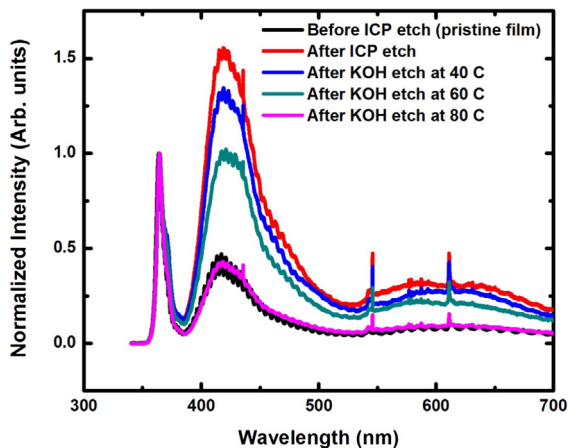


Fig. 5. Room-temperature PL measurement of GaN NWs. The pristine film before ICP etching (black line); after ICP etching (red line); and post-ICP KOH etching for 10 min at 40 °C (blue line), 60 °C (green line) and 80 °C (purple line). All the graphs are normalized by the near-band edge (355 nm) emission intensity. (For interpretation of the references to color in this figure legend, the reader is referred to the web version of this article.)

#### 3.1. Wet etching temperatures

The samples were etched for 10 min in a 10% KOH in deionized water (DIW) solution at 40 °C, 60 °C and 80 °C. PL measurements were conducted before and after KOH etching as well as on the control sample (pristine GaN film). In Fig. 5, intensities are normalized with respect to peaks at near-band edge (NBE) of 355 nm. Surface defects are created during the ICP etch, which are non-radiative recombination centers, results in the decreasing of the NBE emission compared to the impurity-related PL peaks at 420 nm and 600 nm. The subsequent KOH etch removes the ICP-damaged layers from the sidewall surfaces and remarkably reduces the surface non-radiative recombination centers density. After etching at 80 °C, the overall shape of the PL spectrum of GaN NW surface resembles that of the pristine GaN film surface. Similar results also observed and reported on by Q. Li et al. [9].

#### 3.2. Wet etching solvents

The 10% KOH in DIW etchant used above shows the improvement of PL intensity at 80 °C. However, the KOH in DIW shows aggressive etching of the a-plane of GaN, leading to an anisotropic etching profile as shown in the first column of Fig. 6. To address this issue, three different types of etch baths, namely 10% KOH in DIW, isopropanol (IPA) and ethylene glycol (EG), were studied in order to find a truly isotropic etch, one that is more controllable when used in batch fabrication.

All three groups were studied under the same conditions: 10 min etching at 80 °C. PL measurements were conducted after treatment. These results are similar to those shown in Fig. 5 (purple line). SEM images (Fig. 6) reveal different etching rates of different facets: for the top surfaces (c-plane) of GaN NWs, etching was not observable for all three cases. The sidewalls of the NWs (a-plane and m-plane) were found to be more easily attacked by KOH.

Generally speaking, the a-plane is less stable than m-plane due to a higher surface energy [21,22], so the etch rate is faster on a-plane than on the m-plane. SEM images (Fig. 6) show NWs disconnected at several points after etching with KOH in DIW, while m-plane NWs remain the same. Thus, we conclude KOH in DIW etches a-plane much faster than the other solutions. A high reaction rate is not favorable in achieving the smooth etched surfaces [23,24]. An organic solvent addition, such as IPA or EG, slows down the a-plane etching process and making it comparable in rate to m-plane etching in order to achieve “isotropic” etching. The organic solvent contained in the solution plays an important role in the etching process. The organic molecules will selectively adhere to some crystallographic planes (a-plane in our case), thereby hindering the access of etching agent (KOH) and slowing down the corresponding plane's etching rate. KOH in IPA etching shows an improvement in the isotropy of the etch process. IPA can slow down the etch rate of a-plane. However, it still etches faster than the m-plane. KOH in EG etching shows the most isotropic result since both a-plane and m-plane end up with the same NW width. Both the first and second

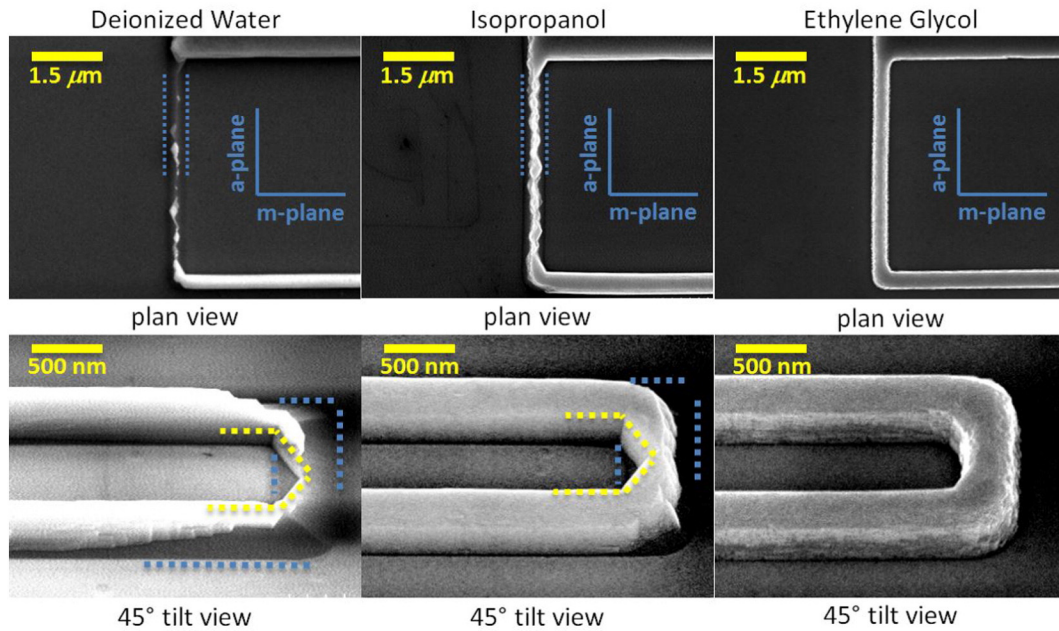


**Fig. 6.** SEM images of NWs after KOH in different solvents. The first row indicates the a-plane and m-plane wires under study. The second row shows the conjoined parts. This is a short a-plane NW connects two m-plane NWs. For DIW and IPA solvents, a-plane NWs were over-etched and disconnected after treatment. Blue dash lines indicate the original NW sidewall positions before the treatment. Yellow dash lines indicate that the final sidewall position after treatment. The m-planes replaced the original a-plane at the inner loop of the part because of a higher etch rate on the a-plane (in contrast to the m-plane.) For the EG solvent, NWs were not severely etched after the treatment. This result shows that the KOH in EG solvent is the best candidate for isotropic etching among the three explored. (For interpretation of the references to color in this figure legend, the reader is referred to the web version of this article.)

columns of Fig. 6 highlight the original NW sidewalls before treatment by blue dashed lines. It is obvious that the a-plane etches faster than m-plane NWs in DIW and IPA. The high magnification image of the

90° bend parts proves this fact. The inner side of the NWs is etched to m-planes with 120° inter-planar angles between them. This is highlighted by the yellow dashed line in these figures. These results

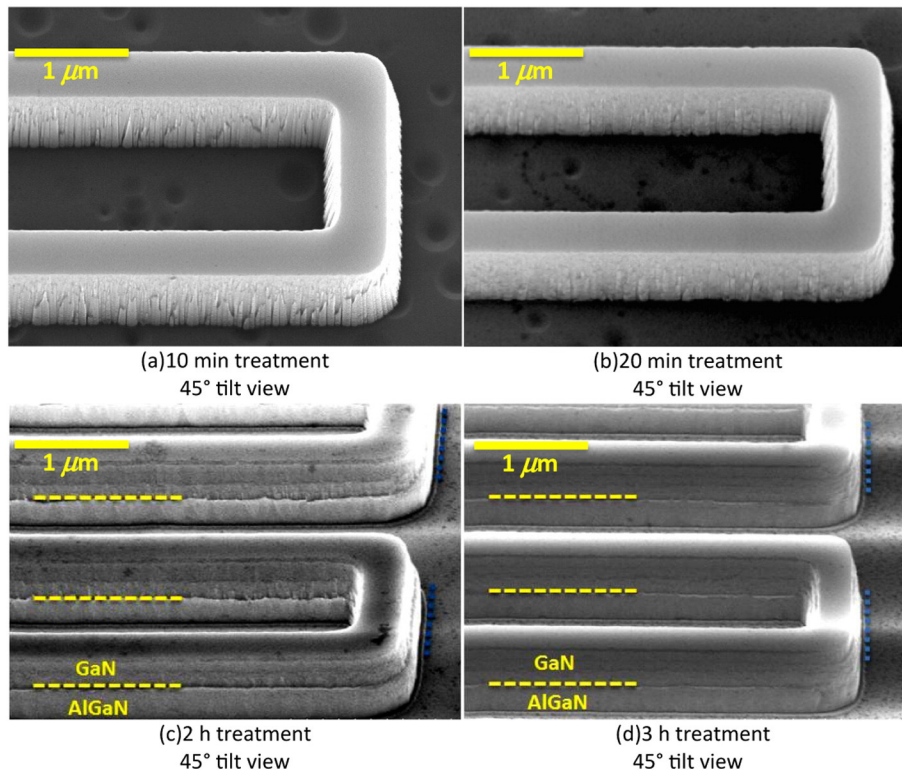


**Fig. 7.** SEM images of NWs after KOH in EG treatments. (a)–(d) correspond to different etching times from 10 min to 3 h under condition of 10% KOH in EG at 80 °C. Blue dash lines in (c) and (d) indicate the original NW sidewall position before the treatment. Yellow dash lines in (c) and (d) indicate the interface between GaN and AlGaN layers after treatment. (For interpretation of the references to color in this figure legend, the reader is referred to the web version of this article.)

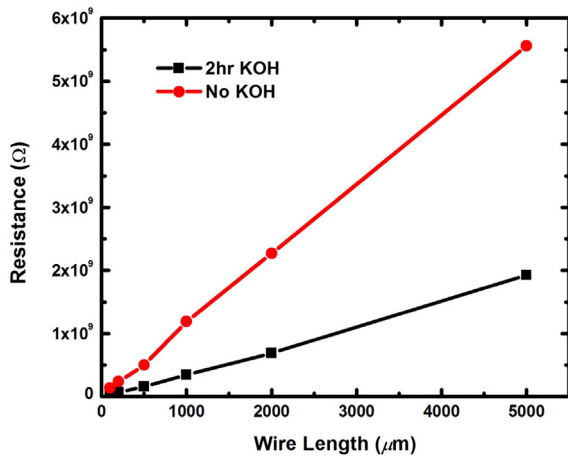


Fig. 8. Electrical behavior with UV assistance of NW before and after KOH treatment.

show that KOH in EG solvent is the best candidate for an isotropic etching for GaN.

### 3.3. Wet etching time

A series of studies of etching times from 10 min to 5 h based on the optimized condition of 10% KOH in EG at 80 °C were conducted. SEM images were taken to observe the NW sidewall surface roughness changes with the increasing etching time. Fig. 4 shows the control group without wet etching treatment, and sidewalls were rough created by plasma bombardment can be clearly seen. Fig. 7 shows a set of SEM images of NW sidewalls after wet etching of 10 min, 20 min, 2 h, and 3 h. The NWs had similar surface morphology with etching times greater than 3 h etching. Both 2 h and 3 h of etching show smooth sidewalls. Comparing Figs. 4 and 7(a), we conclude KOH goes into the deep trenches to widening them and causing the vertical textures to become more pronounced at the beginning of the wet etching. After that, the horizontal textures and steps on the tapered sidewall become visible. The horizontal and vertical texture “cut” the sidewalls into “brick-like” blocks (Fig. 7(b)). These convex block textures are attacked by KOH with further wet etching and decreases the size into smaller convex spots (Fig. 7(c)). After 3 h of etching, the convex structures largely disappeared, ending up with smooth sidewalls (Fig. 7(d)). In Fig. 7(c), (d), the interface layer, highlighted with yellow dash lines, of GaN and AlGaN are identified easily on the smooth sidewall. The original sidewall's position before wet etching can be determined by a KOH resistive nucleation layer as highlighted with blue dash lines.

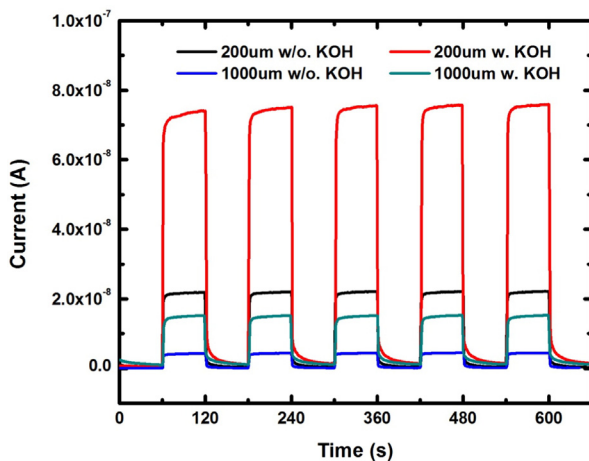


Fig. 9. UV photocurrent transient measurement of 200 μm and 1000 μm long NWs with and without KOH treatment.

### 3.4. Electrical characterization

The electrical properties of the no KOH treatment control group NWs and a 2 h KOH etched NWs with different lengths were studied. I–V measurements were conducted under UV (355 nm wavelength, 48 μW/cm<sup>2</sup> intensity) illumination. Due to the high resistivity of intrinsic GaN, dark currents measured in the pA range (from 10 pA to 100 pA). With UV excitation, resistances tend to increase with increasing NW length, shown in Fig. 8. The KOH treated NWs show lower resistance compared to those no KOH treated NWs at the same length under UV excitation. This enhancement becomes more significant as the NW length decreases. This phenomenon can be explained either by the suppression of the non-irradiative recombination process due to surface improvement or the surface treatment may lead to a lower barrier resistance and form the ideal ohmic contacts.

UV photocurrent measurements were conducted with 200 μm and 1000 μm NWs. For both lengths, NWs with and without KOH wet etching samples compared. The same UV source intensity and voltage biases were used for 5 cycles, 2 min for each cycle (1 min UV on and 1 min off). Fig. 9 shows the response of the NWs' conductance to this cycle. Note: the NW is almost insulating without UV exposure. For the same dimension, surface-treated NWs show almost 3 times higher current under UV exposure. Furthermore, the UV response is proven to be repeatable and reliable over multiple cycles.

## 4. Conclusions

In this study, we were able to reliably and reproducibly fabricate different lengths of alignment-free, horizontal nanowire arrays for various applications. Stepper lithography, ICP etching and KOH wet etching techniques were used to ensure mass production capability and competitive performance to conventional bottom-up nanowires. Different wet etching temperatures, solvents, and times were explored for surface improvement of NWs. PL, SEM and I–V characterization were used to show wet etching is necessary for optimal GaN NW devices. On the basis of our experimental results, this NW fabrication method shows promise, potentially enabling mass production of sensors, optical and power devices based on single NW structures. The top-down approach described here enables GaN NW and SMW to be integrated with LEDs, micro-pumps, micro heaters to provide useful sensor structures. Many sensors (chemical, gas and biology) using bottom-up GaN NWs can be benefit from the top-down approach.

## References

- [1] B. Gil, Group III Nitride Semiconductor Compounds: Physics and Applications, Clarendon Press, 1998.
- [2] V. Dobrokhotov, D. McIlroy, M.G. Norton, A. Abuzir, W. Yeh, I. Stevenson, et al., Principles and mechanisms of gas sensing by GaN nanowires functionalized with gold nanoparticles, *J. Appl. Phys.* 99 (2006) 104302.
- [3] W. Lim, J. Wright, B. Gila, J.L. Johnson, A. Ural, T. Anderson, et al., Room temperature hydrogen detection using Pd-coated GaN nanowires, *Appl. Phys. Lett.* 93 (2008) 072109–072109-3.
- [4] J. Wright, W. Lim, B. Gila, S. Pearson, J.L. Johnson, A. Ural, et al., Hydrogen sensing with Pt-functionalized GaN nanowires, *Sensors Actuators B Chem.* 140 (2009) 196–199.
- [5] A.A. Talin, G.T. Wang, E. Lai, R.J. Anderson, Correlation of growth temperature, photoluminescence, and resistivity in GaN nanowires, *Appl. Phys. Lett.* 92 (2008) 093105.
- [6] Y. Sun, R.A. Graff, M.S. Strano, J.A. Rogers, Top-down fabrication of semiconductor nanowires with alternating structures along their longitudinal and transverse axes, *Small* 1 (2005) 1052–1057.
- [7] X.T. Vu, J.F. Eschermann, R. Stockmann, R. GhoshMoulick, A. Offenhäusser, S. Ingebrandt, Top-down processed silicon nanowire transistor arrays for biosensing, *Phys. Status Solidi A* 206 (2009) 426–434.
- [8] D. Paramanik, A. Motayed, G.S. Aluri, J.-Y. Ha, S. Krylyuk, A.V. Davydov, et al., Formation of large-area GaN nanostructures with controlled geometry and morphology using top-down fabrication scheme, *J. Vac. Sci. Technol. B* 30 (2012) 052202.
- [9] Q. Li, K.R. Westlake, M.H. Crawford, S.R. Lee, D.D. Koleske, J.J. Figiel, et al., Optical performance of top-down fabricated InGa/GaN nanorod light emitting diode arrays, *Opt. Express* 19 (2011) 25528–25534.

- [10] Q. Li, J.B. Wright, W.W. Chow, T.S. Luk, I. Brener, L.F. Lester, et al., Single-mode GaN nanowire lasers, *Opt. Express* 20 (2012) 17873–17879.
- [11] Y. Cui, Q. Wei, H. Park, C.M. Lieber, Nanowire nanosensors for highly sensitive and selective detection of biological and chemical species, *Science* 293 (2001) 1289–1292.
- [12] P. Offermans, M. Crego-Calama, S.H. Brongersma, Gas detection with vertical InAs nanowire arrays, *Nano Lett.* 10 (2010) 2412–2415.
- [13] G. Sberveglieri, C. Baratto, E. Comini, G. Faglia, M. Ferroni, A. Ponzoni, et al., Synthesis and characterization of semiconducting nanowires for gas sensing, *Sensors Actuators B Chem.* 121 (2007) 208–213.
- [14] C.-Y. Wang, L.-Y. Chen, C.-P. Chen, Y.-W. Cheng, M.-Y. Ke, M.-Y. Hsieh, et al., GaN nanorod light emitting diode arrays with a nearly constant electroluminescent peak wavelength, *Opt. Express* 16 (2008) 10549–10556.
- [15] G.S. Aluri, A. Motayed, A.V. Davydov, V.P. Oleshko, K.A. Bertness, N.A. Sanford, et al., Methanol, ethanol and hydrogen sensing using metal oxide and metal (TiO<sub>2</sub>-Pt) composite nanoclusters on GaN nanowires: a new route towards tailoring the selectivity of nanowire/nanocluster chemical sensors, *Nanotechnology* 23 (2012) 175501.
- [16] G.S. Aluri, A. Motayed, A.V. Davydov, V.P. Oleshko, K.A. Bertness, N.A. Sanford, et al., Highly selective GaN-nanowire/TiO<sub>2</sub>-nanocluster hybrid sensors for detection of benzene and related environment pollutants, *Nanotechnology* 22 (2011) 295503.
- [17] C.-P. Chen, A. Ganguly, C.-Y. Lu, T.-Y. Chen, C.-C. Kuo, R.-S. Chen, et al., Ultrasensitive in situ label-free DNA detection using a GaN nanowire-based extended-gate field-effect-transistor sensor, *Anal. Chem.* 83 (2011) 1938–1943.
- [18] R. Chen, C. Lu, K. Chen, L. Chen, Molecule-modulated photoconductivity and gain-amplified selective gas sensing in polar GaN nanowires, *Appl. Phys. Lett.* 95 (2009) 233119.
- [19] J.L. Johnson, Y. Choi, A. Ural, W. Lim, J. Wright, B. Gila, et al., Growth and characterization of GaN nanowires for hydrogen sensors, *J. Electron. Mater.* 38 (2009) 490–494.
- [20] G. Liu, D.A. Lowy, A. Kahrim, C. Wang, Z. Dilli, N. Kratzmeier, et al., A low cost micro-heater for aerosol generation applications, *Microelectron. Eng.* 129 (2014) 46–52.
- [21] J.E. Northrup, J. Neugebauer, Theory of GaN (10 1̄ 0) and (11 2̄ 0) surfaces, *Phys. Rev. B* 53 (1996) R10477.
- [22] Q. Sun, C.D. Yerino, B. Leung, J. Han, M.E. Coltrin, Understanding and controlling heteroepitaxy with the kinetic Wulff plot: a case study with GaN, *J. Appl. Phys.* 110 (2011) 053517.
- [23] I. Zobel, I. Barycka, K. Kotowska, M. Kramkowska, Silicon anisotropic etching in alkaline solutions IV: the effect of organic and inorganic agents on silicon anisotropic etching process, *Sensors Actuators A Phys.* 87 (2001) 163–171.
- [24] I. Zobel, M. Kramkowska, The effect of isopropyl alcohol on etching rate and roughness of (1 0 0) Si surface etched in KOH and TMAH solutions, *Sensors Actuators A Phys.* 93 (2001) 138–147.